2019 American Control Conference (ACC)
Philadelphia, PA, USA, July 10-12, 2019

Theoretical foundations for layered architectures and speed-accuracy tradeoffs in sensorimotor control

Yorie Nakahira[1], Quanying Liu[1], Natalie Bernat[1], Terry Sejnowski[2], John Doyle[1]

***Abstract*— Nervous systems sense, communicate, compute, and actuate movement, using distributed hardware with tradeoffs in speed and accuracy. The resulting sensorimotor control is nevertheless remarkably fast and accurate due to highly effective layered architectures. However, such architectures have received little attention in neuroscience due to the lack of theory that connects the system and hardware level speed-accuracy tradeoffs. In this paper, we present a theoretical framework that connects the speed-accuracy tradeoffs of sensorimotor control and neurophysiology. We characterize how the component SATs in spiking neuron communication and their sensory and muscle endpoints constrain the system SATs in both stochastic and deterministic models. The results show that appropriate speed-accuracy diversity at the neurons/muscles levels allow nervous systems to improve the speed and accuracy in control performance despite using slow or inaccurate hardware. Then, we characterize the fundamental limits of layered control systems and show that appropriate diversity in planning and reaction layers leads to *both* fast and accurate system despite being composed of slow or inaccurate layers. We term these phenomena "Diversity Sweet Spots." The theory presented here is illustrated in a companion paper, which introduces simple demos and a new inexpensive and easy-to-use experimental platform.**

I. INTRODUCTION

To concretely illustrate speed-accuracy tradeoffs (SATs) in layered architectures, consider riding a mountain bike down a twisting bumpy trail. There is an obvious tradeoff between speed down the trail, and accuracy in staying on it and not crashing. But how exactly is the rider's nervous system organized to allow experts to have extremely robust performance despite complex, uncertain environments and despite implementation in a hardware level of spiking neurons that is distributed, sparse, quantized, delayed, and/or saturating? A crucial strategy is the evolution of effective layered architectures that integrate nerves/muscles with diverse speed and accuracy as well as high-layer planing that track the trail with the low-layer reaction that handles bumps and is largely unconscious and automatic [1], [2].

Fig. 1 is a block diagram of a minimal and highly abstract model of the system level components involved in the biking problem, which includes sensing, communication, computation, and actuation. This is the same diagram presented in a companion paper, which considers a video game version of the biking problem [3]. The plant **P** consists of bike and rider and is (possibly marginally) unstable, and must track a reference trail changes $r(t)$ with small error despite unseen bumps $w(t)$. Each box is designated by its function and either senses and communicates (vision **V**, muscle spindle sensor **S**), actuates (muscle **M**) or computes a control action (high layer tracking **H** and low layer reflex **L**). Each box can have quantization, delay, saturation and/or stochastic or deterministic noise, depending on the hardware or model details. Vision gives the rider advance warning of the trail ahead, which is modeled here by a (variable) delay **T** between r and the plant that depends on speed, terrain, and the trail shape.

The theoretical challenge addressed here is to provide a framework that can compute optimally robust controllers for problems like Figure 1 with realistic models for uncertainties and component limitations. We provide insights using analytic formulas for important special cases and scalable algorithms for general problems. Our theory shows that appropriate speed-accuracy diversity at the neurons/muscles levels allow nervous systems to improve the speed and accuracy in control performance despite using slow or inaccurate hardware. Similarly, layering diverse controllers can create systems that are *both* fast *and* accurate despite being built from individual layers that are not. We term these phenomena "diversity sweet spots" (DSSs). Finally, we show that the key insights are remarkably robust to the assumptions (average vs. worst-case, stochastic vs. deterministic) in the extended version of our paper [4] and discuss biological plausibility of our model in our companion paper, which also includes a variety of additional illustrative demos [3].

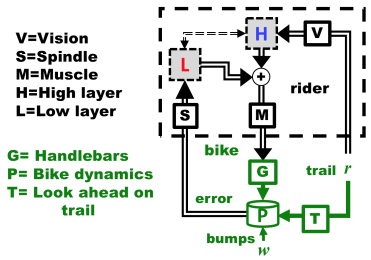

Fig. 1: Basic block diagram of a sensorimotor control model for a mountain bike and rider on a twisting trail with bumps. Each box is a component that communicates (V,S,M) or computes (H,L) using spiking neurons and thus has potentially both delay and quantization. The rider can see the trail ahead and thus has advanced warning T that would depend on speed and terrain, and can be used by the higher layer controller. The bumps are not seen but can crash the bike if not correctly handled by lower layer reflexes.

While modern lifestyles largely shield us from the challenges that shaped our brain's evolution, we see SAT and DSS appear everywhere in neuroscience, though the results are fragmented and incoherent, and even the terminology is not consistent. For example, different types of sensorimotor

978-1-5386-7926-5/$31.00 ©2019 AACC

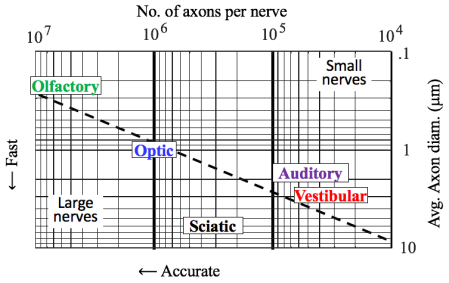

Fig. 2: The large diversity in the composition of selected human cranial and spinal nerves and the resulting speed-accuracy tradeoffs. The dashed line shows a constant total cross-sectional area, which is roughly proportional to the cost to build and maintain a nerve of a given length and is similar across the different nerves, which are otherwise quite different. Our nerve model will translate axon size and number into a biologically realistic delay and data rate, and the theory will then connect this hardware level SAT with system level SATs. This cartoon understates the diversity, both between the same nerve in different individuals, and between the axons within a single nerve, both of which are large and poorly characterized. Adapted from [5]

nerves have extremely diverse size and number (see Figure 2 for selected cranial and spinal nerves). While bundles of axons in most nerves, from optic (vision) to vestibular to sciatic (reflexes) in Figure 2 have similar total cross-sectional areas (roughly proportional to the cost to build and maintain), they have extremely diverse compositions in terms of axon size and number [6]–[9]. As we will show, the limitation in biological resource translates directly into strict tradeoffs in signaling speed (in terms of delay) and accuracy (in terms of the amount of transmittable information), which in turn imposes the system level SATs. Interestingly, most system level SATs, from decisions [10] to reaching (Fitts' law) [11], [12] to sports (baseball, cricket, and soccer) [13], [14] (which perhaps more reflect our evolutionary past), are much less severe than what should be imposed by the component level SATs. Despite this apparent discrepancy, little existing literature paid attention to this issue. This lack of attention is because clarifying this discrepancy requires understanding the rich design tradeoffs and principles from a holistic perspective of both levels, and the two levels are currently treated separately due to the lack of theoretical tools that integrate them. We aims to fundamentally change this situation [15], [16]. As an initial step, in this paper, we show that diversity in the neurons/muscles levels and between planning/reaction layers can de-constrain hardware speed-accuracy constraints for achieving fast *and* accurate sensorimotor performance, shedding lights on the largely overlooked power of DSSs.

Notation: We use $x(t_1 : t_2) = \{x(t_1), x(t_1+1), \cdots, x(t_2)\}$ to denote a truncated sequence. The ℓ_∞ norm of a sequence x is defined as $\|x\|_\infty := \sup_t |x(t)|$. We use $P(x)$ to denote the probability density function of a random variable x, and $P(x|y)$ to denote the conditional probability density function of x given another random variable y. We use $\log(x)$ to denote the logarithm of x in base 2 and $\log_b(x)$ to denote the logarithm of x in base b. We use $\mathbb{Z}/\mathbb{Z}_+$ and $\mathbb{R}/\mathbb{R}_+$ to denote the set of all/non-negative integers and the set of all/non-negative real numbers, respectively.

II. MAIN RESULTS

To clarify the fundamental limits of sensorimotor control imposed by hardware constraints, we present a mathematical framework of robust control involving sensing, communication, and actuation and derive performance bounds. This framework accommodates different assumptions on delay, data rate, and saturation due to hardware limitations in both deterministic worst case and stochastic average case.

In this section, we focus on a worst-case analysis, which produces qualitatively similar results with an average-case analysis. Worst-case analysis is beneficial in its biological plausibility and ease of derivation. In many sensorimotor tasks, there are strict error bounds which cannot be violated: for example, when riding a mountain bike on a cliff, not falling off the cliff is far more critical than minimizing average errors. Moreover, the worst-case framework is also simpler than the average-case: deriving worst-case performance only requires high-school level mathematics and thus has significant potential in education and interdisciplinary research [3], [16].

Below, we summarize the SATs in spike-based neural signaling (Section II-A) and its impact on robust performance for systems whose performance bottleneck lies in the neural signaling (Section II-B–II-C). Closed-form performance bounds are derived for both a basic control system and a layered network with uniform/diverse nerves, and the resulting insights are consistent with those from alternative models/assumptions discussed in the extended version of this paper [4].

A. Component-level SATs

In a sensorimotor feedback loop, sensory information is transmitted by spikes (action potentials) through nerve fibers (axons). The space and metabolic constraints of a nerve limit the number and size of axons that can be built and maintained. These limits lead to SATs in neural signaling [6], [17], [18], and the specific forms of the SATs depend on how the nerves encode information (*e.g.* spike-based, spike-rate encoding). Below, we derive the SATs for spike-based encoding in this section and discuss other alternatives in the extended version of this paper [4].

In a spike-based encoding scheme, information is encoded in the presence or absence of a spike in specific time intervals, analogous to digital packet-switching networks [19], [20]. This encoding method requires spikes to be generated with sufficient accuracy in timing, which has been experimentally verified in multiple types of neuron [21], [22].

To quantify the complex distribution of axon sizes in a single nerve, we can think of a nerve as being made up of several *communication channels*, each containing axons with identical size. We assume that there are m heterogeneous communication channels and index them by $i \in$

$\{1, 2, \cdots, m\}$. We use n_i, ρ_i to denote the number of axons contained in channel i and the radius of axons in channel i, respectively. We use T_i, R_i to denote the delay and data rate (*i.e.* the amount of information in bits that can be transmitted) of channel i, respectively.

When the signaling is precise and noiseless, an axon with achievable firing rate ϕ can transmit ϕ bits of information per unit time. For sufficiently large myelinated axons, the propagation speed $1/T_i$ and firing rate ϕ are both approximately proportional to the axon radius ρ [6], *i.e.*

$$T = \alpha/\rho \qquad\qquad \phi = \beta\rho,$$

where α and β are proportionality constants. Moreover, the space and metabolic costs of a nerve are proportional to its volume [6], and given a fixed nerve length, these costs are proportional to its total cross-sectional area s. Using the above properties, we can show that[1]

$$R_i = \lambda_i T_i \qquad\qquad \sum_{i=1}^{m} \lambda_i = \frac{s\beta}{\pi\alpha} \tag{1}$$

A special case of (1) is when all axons are uniform, *i.e.* when ρ_i are identical for all i. In such a case, we can think of the nerve as a single communication channel with delay $T_s = T_i$ and $R = \sum_{i=1}^{m} R_i$ satisfying

$$R = \lambda T_s \qquad\qquad \lambda = \frac{s\beta}{\pi\alpha}. \tag{2}$$

We refer to nerves that have a diverse distribution of axon diameters as *diverse nerves* and those with a uniform distribution as *uniform nerves* for the rest of the paper.

B. System-level SATs

We consider a sensorimotor control model with the system dynamics

$$x(t+1) = ax(t) + w(t) + u(t)$$

where $x(t) \in \mathbb{R}$ is the state, $w(t) \in \mathbb{R}$ is the disturbance, $u(t) \in \mathbb{R}$ is the control action. We assume that the disturbance is ∞-norm bounded and, without loss of generality, $\|w\|_\infty \leq 1$. The control action is generated through a feedback loop, which is constrained by data rate, delay, and/or saturation. The control action is generated by a controller K_t:

$$\begin{aligned} &\mathcal{I}_t = \{x(0:t), w(0:t+T_a), s(0:t-1)\} \\ &[s_1(t), s_2(t), \cdots, s_m(t)] = K_t(\mathcal{I}_t) \end{aligned} \tag{3}$$

and m quantizers:

$$u(t) = \sum_{i=1}^{m} Q_i(s_i(t - T_i - T_c)), \tag{4}$$

Here, the controller can access the disturbance information with an advanced warning of T_a, but its command is put into action with a delay of $T_i + T_c$, where T_i is the signaling delay satisfying the SATs (1) or (2), and $T_c \geq 0$ is other internal delays such as computation. Each quantizer Q_i has rate R_i, so the data rate $R = \sum_{i=1}^{m} R_i$ is the number of bits per sampling interval that can be transmitted from the sensors to the actuators in the feedback loop. We additionally assume that the data rate is minimum stabilizing, *i.e.* $R > \log(|a|)$ [23]. We pose the robust control problem as follows:

$$\inf \sup_{\|w\|_\infty \leq 1} \|x\|_\infty, \tag{5}$$

where the infimum is taken over the control policies of the form (3) and (4). This robust control problem is motivated by sensorimotor tasks such as driving and riding a mountain bike. In such tasks, $x(t)$ models the error between desired and actual trajectories; $u(t)$ models the control action taken by the sensorimotor system; and $w(t)$ models environmental noise and/or uncertainty in the desired trajectory. For more detail, see Figure 1 and our companion paper on experiments [3].

The following lemma characterizes the performance limits on system robustness.[1]

Lemma 1: The minimal state-deviation (5) is

$$\sum_{h=1}^{\infty} |a^{h-1}| \frac{1}{2^{\mathcal{R}(h)}}, \tag{6}$$

where $\mathcal{R} : \mathbb{Z}_+ \to \mathbb{R}_+$ is a function of $h \in \mathbb{Z}_+$ given by

$$\mathcal{R}(h) := \sum_{i=1}^{m} \max\{0, h - T_i - T_c + T_a\} R_i.$$

Formula (6) can be used to characterize the impact of instability. Specifically, the minimal state-deviation (5) of an unstable system with $T_c - T_a = 0$ and uniform nerves (*i.e.* $|a| \geq 1$, $m = 1$, and $T = T_1$) is given by[2]

$$\sup_{\|w\|_\infty \leq 1} \|x\|_\infty \geq \sum_{i=1}^{T} |a^{i-1}| + |a^T| \frac{1}{2^R - |a|}, \tag{7}$$

where the equality can be attained with minimal control effort

$$\sup_{\|w\|_\infty \leq 1} \|u\|_\infty = \left(|a^T| + \frac{|a^T|}{2^R - |a|}\right)\left(1 - \frac{1}{2^R}\right). \tag{8}$$

The control policy that achieves (7) and (8) is given in [15]. Interestingly, this optimal controller resembles predictive coding in neural signaling (see [4] for more detail).

Note that although unstable systems do not have a tradeoff between minimizing state-deviation and minimizing control effort, this property does not hold for stable systems, *i.e.* $|a| < 1$. In particular, the minimal state-deviation (5) of a stable system subject to $\|u(t)\|_\infty \leq \ell$ is given by[1]

$$\begin{cases} \displaystyle\sum_{i=1}^{T} |a^{i-1}| + |a^T| \frac{1}{2^R - |a|} & \text{if } \ell \leq |a| \frac{2^R - 1}{2^R - |a|} \\ \displaystyle\sum_{i=1}^{T} |a^{i-1}| + |a^T| \frac{1 - \ell}{1 - |a|} & \text{otherwise.} \end{cases}$$

[1] Due to space constraints, we present a more detailed derivation in the extended version of this paper [4].

[2] With a light abuse of notation, we denote $\sum_{i=t_1}^{t_2} f(i) = 0$ if $t_2 < t_1$.

An important special case is the system with $a = 1$, which reduces to the setting of our driving game experiment and other tasks such as riding a mountain bike [3] or eye movements [15], [16]. If such system is built from uniform nerves, the minimal state-deviation (5) is given by

$$\max(0, T_s + T_c - T_a) + \frac{1}{2^R - 1}. \tag{9}$$

We can interpret the first term as the error due to having delay in the feedback loop (denote as delay error), and the second term as the error due to having limited data rate in the feedback loop (denote as quantization error). Note that the impact of delay and quantization is experimentally verified in our driving game experiments [3].

If the system is built from two types of axons (*i.e.* $m = 2$) and $T_a - T_i = 0$, then (6) reduces to

$$T_1 + \frac{1 - 2^{-R_1(T_2 - T_1)}}{2^{R_1} - 1} + \frac{1}{2^{R_1(T_2-T_1)}} \frac{1}{2^{R_1+R_2} - 1}. \tag{10}$$

We can similarly interpret the first term as the delay error, and the second and third term as the quantization error. Combining (2) and (9), we obtain the system SATs when sensorimotor control is implemented using uniform nerves. Combining (1) and (10) yields the system SATs when sensorimotor control is implemented using diverse nerves.

C. SATs in a layered architecture

Previous sections describe the SATs at the component and system levels. In this section, we derive the SATs for layered architectures. Figure 1 sketches a minimal layered sensorimotor control model composed of higher-layer planning of trajectories and lower-layer reflex compensation to reject disturbance. The control commands from both layers are put into action by muscles. Specifically, we consider the system dynamics

$$x(t+1) = ax(t) + u(t) + r(t) + w(t), \tag{11}$$

where $r(t)$ models the changes in the desired trajectory, and $w(t)$ models the disturbance. We assume that $r(t), w(t)$ are ∞-norm bounded, and without loss of generality, $\|r\|_\infty \leq 1$, $\|w\|_\infty \leq \epsilon$.

We consider two specific ways of layering: with or without shared information between the two controllers. The layered control system with shared information is defined by

$$\begin{aligned} \mathcal{I}_t &= \{x(0:t), w(0:t), r(0:t+T_a)\} \\ u_h(t) &= H(\mathcal{I}_{t-T_h}, u(0:t-1)) \\ u_\ell(t) &= L(\mathcal{I}_{t-T_\ell-T_c}, u(0:t-1)) \\ u(t) &= Q_m(Q_\ell(u_\ell(0:t)), Q_h(u_h(0:t))). \end{aligned} \tag{12}$$

Here, H is a high-layer planner, L is a lower-layer disturbance compensator. The accuracy constraint of each controller is modeled by quantizers Q_ℓ/Q_h with data rates R_ℓ/R_h. The commands from both controllers are put into action by the muscles, whose accuracy are modelled by the quantizer Q_m with data rate R_m. The layering without shared information is defined by

$$\begin{aligned} u_h(t) &= H(r(0:t-T_h+T_a), u(0:t-1)) \\ u_\ell(t) &= L(w(0:t-T_\ell-T_c), u(0:t-1)) \\ u(t) &= Q_m(Q_\ell(u_\ell(0:t)), Q_h(u_h(0:t))). \end{aligned} \tag{13}$$

We pose the robust control problem as follows:

$$\inf \sup_{\|w\|_\infty \leq \epsilon, \|v\|_\infty \leq 1} \|x\|_\infty, \tag{14}$$

where the infimum is taken over the control policy with shared information (12) or that without shared information (13). Let $\bar{R}_\ell$ and $\bar{R}_h$ be defined by

$$\begin{aligned} \bar{T}_\ell &:= T_\ell + T_c & \bar{R}_\ell &:= \min(R_\ell, R_m) \\ \bar{T}_h &:= T_h - T_a. & \bar{R}_h &:= \min(R_h, R_m) \end{aligned}$$

In the case with shared information, the minimum state-deviation (14) achievable by controller (12) is

$$\left\{ \sum_{i=1}^{\bar{T}_\ell} |a^{i-1}| + \sum_{\tau=\bar{T}_\ell+1}^{\infty} \frac{|a^{\tau-1}|}{2^{\bar{R}_\ell(\tau-\bar{T}_\ell)+\bar{R}_h \max(0,\tau-\bar{T}_h)}} \right\} (1+\epsilon) \tag{15}$$

The proof of (15) is a trivial extension of Lemma 1. When $a = 1$, (15) equals

$$\left\{ \bar{T}_\ell + \frac{1 - 2^{-\bar{R}_\ell(\bar{T}_h - \bar{T}_\ell)}}{2^{\bar{R}_\ell} - 1} + \frac{1}{2^{\bar{R}_\ell(\bar{T}_h-\bar{T}_\ell)}} \frac{1}{2^{\bar{R}_\ell+\bar{R}_h} - 1} \right\} (1+\epsilon). \tag{16}$$

In the case without shared information, the state-deviation (14) achievable by the controller (13) is lower-bounded by

$$\left\{ \sum_{i=1}^{\bar{T}_\ell} |a^{i-1}| + \frac{|a^{\bar{T}_\ell}|}{2^{\bar{R}_\ell} - |a|} \right\} \epsilon + \sum_{i=1}^{\max\{0,\bar{T}_h\}} |a^{i-1}| + \frac{|a^{\max\{0,\bar{T}_h\}}|}{2^{\bar{R}_h} - |a|}. \tag{17}$$

The performance limit (17) is a simple generalization of the results of [15, Section IV.C]. In the next section, we use these formulas to explore the benefit of axon diversity at the nerve/muscle level and between planning/reaction layers.

III. IMPLICATIONS

The results presented in Section II show our first steps towards integrating the previously disjoint fields of neurophysiology and sensorimotor control. This theoretical framework offers a more coherent view of the rich and complex design space of the sensorimotor nervous system. It shows how a sensorimotor control system can achieve fast and accurate system performance through effective architectures, which help overcome the fundamental limitations incurred by components that may be slow or inaccurate.

Attaining optimal/robust performance requires two conditions: optimal hardware components and optimal control/communication policies. To achieve the former condition, hardware needs to be built with appropriate speed and accuracy so that neither the delay costs nor the quantization costs overwhelm the system performance. Although the

hardware SATs inevitably lead to system SATs, appropriate diversity at the nerve/muscle level and planning/reaction layers help achieve less stringent system SATs.

To achieve the latter condition, our results indicate that certain structures of optimal controllers allow for optimal control/communication policy. Interestingly, the seemingly cryptic patterns of feedback and feedforward pathways seen in vertebrate nervous systems resemble optimal controllers for delayed/quantized systems, as well as those from the System Level Synthesis (SLS) method [24] for distributed/localized systems (see [4] for more detail).

A. Diversity sweet spots in SATs optimize performance

The framework developed in section II-B can further describe the effects of diversity in neural composition on performance. For the system with uniform nerves, we associate its system SATs with the delay versus quantization costs in (9). For systems with diverse nerves, we associate its system SATs with the delay cost T_1 in (10), *i.e.* the errors before the first packet arrives, and the quantization cost $(1-2^{-R_1(T_2-T_1)})/(2^{R_1}-1)+1/(2^{R_1(T_2-T_1)}(2^{R_1+R_2}-1)$. Figure 3 right compares the resulting SATs for systems with uniform nerves and diverse nerves. From Figure 3, systems with diverse nerves have an improved SAT compared with systems with uniform nerves, suggesting that diversity in nerve composition can achieve the system performance as if uniformly fast and accurate axons are used. We call this phenomenon a *diversity sweet spot* (DSS), to emphasize the trend that, when choosing how to devote resources to a system, it is often better for overall system performance to use diverse components than to devote all resources to either end of a tradeoff.

Similarly, the results of section II-C demonstrate another DSS and the benefit of diversity between layers. Figure 4 (left) compares the performance lower-bounds (17) for the layered system without shared information (11), (13) when the delay and data rate of the higher-layer (T_ℓ, R_ℓ) and those of the lower-layer (T_h, R_h) are allowed to be diverse or are constrained to be uniform, given sufficiently large R_m. The performance gain is especially high when the two layers are heterogeneous, *i.e.* large $T_c - T_a$ (Figure 4), demonstrating the benefit of using diverse nerves between higher and lower layers. A similar DSS can be observed in an alternative setting of shared information, whose performance lower-bound is given by (16). The results suggest that layered architectures of diverse control loops, if well-exploited, help achieve fast and accurate sensorimotor performance despite the speed and accuracy constraints of individual layers. Delving further into this example, we observe diversity in hardware that achieves this optimal system performance. The optimal nerves for (17) with $m = 2$ have consistently small T_ℓ to control the cost of delay, but allows R_h to increase for large advanced warning T_a (Figure 4, right)

It is important to note that the properties we have found to be optimal are indeed observed in nature. As seen in Figure 2, the nerves involved in many sensory modalities have a wide range of size and number of axons, which leads to a wide range of signaling speed and accuracy. Further, the distributions of axons within nerves are highly diverse, especially those involved in sensorimotor control like the optic, vestibular, and sciatic nerves. These observations indicate that a diversely layered control architecture composed of diversely distributed axon sizes is plausible within the limits of observed neurophysiology.

B. SAT in muscle actuation and reaching tasks

In this section, we present another component and system SATs that illustrate the DDS, involving muscle actuation and reaching tasks. We consider a simplified muscle model which includes m motor units, indexed by $i \in \{1, 2, \cdots, m\}$, each associated with a reaction speed and a strength level. We use F_i to denote its strength and assume without loss of generality that $F_1 \leq F_2 \cdots \leq F_m$. Motor units are recruited in ascending order of F_i, so a muscle (at non-transient time) can only generate $m+1$ levels of discrete strength levels: $\sum_{i=1}^{n} F_i,\ n \in \{0, 1, 2, \cdots, m\}$.[1] Because the strength of a motor unit is roughly proportional to its cross-sectional area (myofibril cross-sectional area) [25], given a fixed lengths, the maximum strength of a muscle $\ell = \sum_{i=1}^{m} F_i$ is proportional to its cross-sectional area. This implies that, given a fixed space to build a muscle, its maximum strength does not depend on the specific composition of motor units.

Given a fixed maximum strength ℓ, there is a tradeoff between a muscle's reaction speed and resolution. Specifically, if a motor unit is recruited at time $t = 0$, then its strength $c_i(t)$ raises according to[1]

$$\dot{a}_i(t) = \alpha f_i^p (1 - a_i(t)) - \beta a_i(t), a_i^q(t) = c_i(t) \qquad (18)$$

with the initial condition $c_i(0) = 0$, $f_i = 1/((\gamma/F_i)^{1/q} - 1)$. We set $\alpha = 1, \beta = 1, p = 1$ to be fixed constants given in [8]. Similarly, when a recruited motor unit is released at time $t = 0$ its contraction rate falls according to (18) with $f_i = 0$ and $c_i(0) = F_i$. The relation (18) indicates that the reaction speed of a muscle is an increasing function of F_i.Constrained by $\ell = \sum_{i=1}^{m} F_i$, a muscle can be built from many motor units with small strengths or a few motor units with large strengths. In the former case, the muscle has better resolution but slow reaction speed, while in the latter case, the muscle has fast reaction speed but coarser resolution.

This component SAT leads to a system SAT in a reaching task. Consider reaching a hand towards a target of width D located at a fixed distance (a task typically associated with Fitts' Law). In this task, the reaching time provides a measure of speed and the target width is a measure of accuracy. Figure 5 shows this maximum reaching time (speed) given a fixed target width (accuracy). When we naively build a muscle using uniform motor units, the SAT has a linear form, which is inconsistent with standard experiments. However, *diversity* in motor units achieves a logarithmic SAT, yielding a DSS in which both speed and accuracy can be achieved. Although this logarithmic SAT has been observed in the context of Fitts' law, the connection between the logarithmic nature of Fitts' law and the notion of DSS has not previously been made.

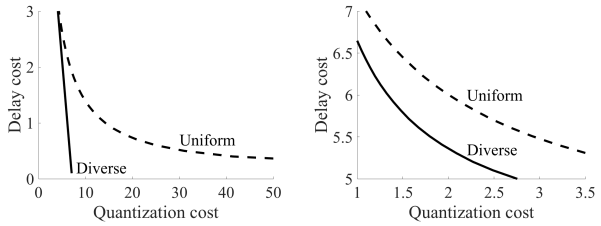

Fig. 3: The benefit of diversity at the nerve level (left) and between layers (right). We use $m = 1$ for uniform nerves and $m = 2$ for diverse nerves, and we set $s\beta/(\pi\alpha) = 1$ and $T_i - T_a = 0$. In both cases, diversity enables the system to improve its system SAT in sensorimotor control performance. Adapted from [5].

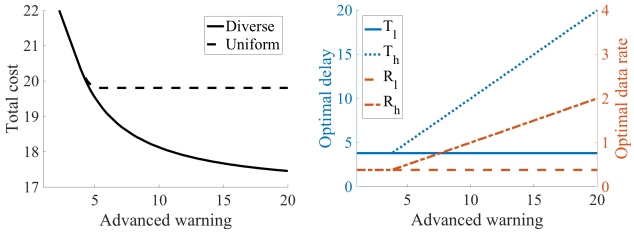

Fig. 4: The benefit of nerve diversity in layered architectures. The left shows the minimum state-deviation (17) for varying advanced warning T_a in the case when *diverse* delays and data rates of L and H are allowed, versus the case when only *uniform* delays and data rates are permitted (*i.e.* $R_\ell = R_h$ and $T_\ell = T_h$). Other parameters are set to be $R_\ell = 0.1T_s$, $R_h = 0.1T_h$, and $T_c = 10$. The right shows the resulting optimal delays and data rates for the diverse case. Adapted from [5].

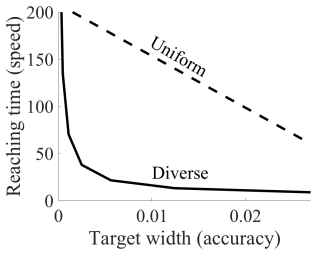

Fig. 5: The SAT in a reaching task imposed by the SAT of a muscle with uniform versus diverse motor units. For a fixed sensorimotor control sampling interval, an upper bound $\bar{F}$ on the strength of recruitable motor units is obtained from the target width (accuracy requirement) using (18). Then, from $\bar{F}$, the reaching time is computed using (18) for the case of recruiting all motor units with strength below $\bar{F}$. Adapted from [26].

REFERENCES

[1] N. Lan, V. C. Cheung, and S. C. Gandevia, "Neural and computational modeling of movement control," *Frontiers in computational neuroscience*, vol. 10, p. 90, 2016.

[2] J. C. Doyle and M. Csete, "Architecture, constraints, and behavior," *Proceedings of the National Academy of Sciences*, vol. 108, no. Supplement 3, pp. 15624–15630, 2011.

[3] Q. Liu, Y. Nakahira, A. Mohideen, S. Choi, and J. C. Doyle, "A experimental platform to study the speed/accuracy tradeoffs and layered architectures in human sensorimotor control." Accepted to the 2019 American Control Conference.

[4] Y. Nakahira, Q. Liu, N. Bernat, T. Sejnowski, and J. C. Doyle, "Theoretical foundations for layered architectures and speed-accuracy tradeoffs in sensorimotor control (extended version)." http://users.cms.caltech.edu/ ynakahir/.

[5] "Diversity sweet spots in layered architectures and speed-accuracy trade-offs in sensorimotor control." In preparation.

[6] P. Sterling and S. Laughlin, *Principles of neural design*. MIT Press, 2015.

[7] C. J. De Luca and Z. Erim, "Common drive of motor units in regulation of muscle force," *Trends in neurosciences*, vol. 17, no. 7, pp. 299–305, 1994.

[8] V. Brezina, I. V. Orekhova, and K. R. Weiss, "The neuromuscular transform: the dynamic, nonlinear link between motor neuron firing patterns and muscle contraction in rhythmic behaviors," *Journal of neurophysiology*, vol. 83, no. 1, pp. 207–231, 2000.

[9] S. Li, C. Zhuang, M. Hao, X. He, J. C. Marquez Ruiz, C. M. Niu, and N. Lan, "Coordinated alpha and gamma control of muscles and spindles in movement and posture," *Frontiers in computational neuroscience*, vol. 9, p. 122, 2015.

[10] R. P. Heitz, "The speed-accuracy tradeoff: history, physiology, methodology, and behavior," *Frontiers in neuroscience*, vol. 8, p. 150, 2014.

[11] P. M. Fitts and J. R. Peterson, "Information capacity of discrete motor responses.," *Journal of experimental psychology*, vol. 67, no. 2, p. 103, 1964.

[12] R. W. Soukoreff and I. S. MacKenzie, "Towards a standard for pointing device evaluation, perspectives on 27 years of fitts law research in hci," *International journal of human-computer studies*, vol. 61, no. 6, pp. 751–789, 2004.

[13] J. Freeston and K. Rooney, "Throwing speed and accuracy in baseball and cricket players," *Perceptual and motor skills*, vol. 118, no. 3, pp. 637–650, 2014.

[14] R. van den Tillaar and A. Ulvik, "Influence of instruction on velocity and accuracy in soccer kicking of experienced soccer players," *Journal of motor behavior*, vol. 46, no. 5, pp. 287–291, 2014.

[15] Y. Nakahira, N. Matni, and J. C. Doyle, "Hard limits on robust control over delayed and quantized communication channels with applications to sensorimotor control," in *Decision and Control (CDC), 2015 IEEE 54th Annual Conference on*, pp. 7522–7529, IEEE, 2015.

[16] J. Doyle, Y. Nakahira, Y. P. Leong, E. Jenson, A. Dai, D. Ho, and N. Matni, "Teaching control theory in high school," in *Decision and Control (CDC), 2016 IEEE 55th Conference on*, pp. 5925–5949, IEEE, 2016.

[17] J. A. Perge, K. Koch, R. Miller, P. Sterling, and V. Balasubramanian, "How the optic nerve allocates space, energy capacity, and information," *Journal of Neuroscience*, vol. 29, no. 24, pp. 7917–7928, 2009.

[18] J. A. Perge, J. E. Niven, E. Mugnaini, V. Balasubramanian, and P. Sterling, "Why do axons differ in caliber?," *Journal of Neuroscience*, vol. 32, no. 2, pp. 626–638, 2012.

[19] E. Salinas and T. J. Sejnowski, "Correlated neuronal activity and the flow of neural information," *Nature reviews neuroscience*, vol. 2, no. 8, p. 539, 2001.

[20] K. H. Srivastava, C. M. Holmes, M. Vellema, A. R. Pack, C. P. Elemans, I. Nemenman, and S. J. Sober, "Motor control by precisely timed spike patterns," *Proceedings of the National Academy of Sciences*, vol. 114, no. 5, pp. 1171–1176, 2017.

[21] Z. F. Mainen and T. J. Sejnowski, "Reliability of spike timing in neocortical neurons," *Science*, vol. 268, no. 5216, pp. 1503–1506, 1995.

[22] J. L. Fox, A. L. Fairhall, and T. L. Daniel, "Encoding properties of haltere neurons enable motion feature detection in a biological gyroscope," *Proceedings of the National Academy of Sciences*, p. 200912548, 2010.

[23] G. N. Nair, F. Fagnani, S. Zampieri, and R. J. Evans, "Feedback control under data rate constraints: An overview," *Proceedings of the IEEE*, vol. 95, no. 1, pp. 108–137, 2007.

[24] Y.-S. Wang, N. Matni, and J. C. Doyle, "A system level approach to controller synthesis," *arXiv preprint arXiv:1610.04815*, 2016.

[25] G. Goldspink, "Malleability of the motor system: a comparative approach," *Journal of experimental biology*, vol. 115, no. 1, pp. 375–391, 1985.

[26] "Fitts' law for speed-accuracy trade-off is a diversity sweet spot in sensorimotor control." In preparation.